2025 International Conference on Quantum Photonics, Artificial Intelligence, and Networking (QPAIN)
31 July – 2 August 2025, Rangpur, Bangladesh

2025 International Conference on Quantum Photonics, Artificial Intelligence, and Networking (QPAIN) | 979-8-3315-9694-1/25/$31.00 ©2025 IEEE | DOI: 10.1109/QPAIN66474.2025.11171708

Tversky Loss Mechanisms: A ResUNet Approach to Improving Brain Tumor Segmentation

Md. Rifat Hossen[1], Ekram Hossain[2], Jonayed Al-Faruk[2], Jahin Sultana[3], Md. Bodrul Islam[2], Md. Sarwar Hosain[1]
[1]Dept. of Information and Communication Engineering,
Pabna University of Science and Technology, Pabna, Bangladesh
[2]Dept. of Computer Science and Engineering,
Mymensingh Engineering College, Mymensingh, Bangladesh
[3]Dept. of Computer Science and Engineering,
American International University-Bangladesh, Dhaka, Bangladesh
Email: [1]rifat.pust.ice14@gmail.com, [2]ekramhossain117@gmail.com, [2]jonayedalfaruk211282@gmail.com,
[3]jahinsultana21@gmail.com, [2]mdbodrulislam369@gmail.com, [1]sarwar.ice@pust.ac.bd

***Abstract*—Biomedical imaging exemplifies a modern transdisciplinary collaboration in medicine. Various deep learning and AI techniques can automate tumor segmentation. Brain tumors typically have the poorest prognosis, as most patients succumb once the tumors reach their maximum size. It is crucial to identify and segment the tumor when it is small enough for surgical removal, despite the availability of multiple imaging modalities for tumor segmentation. Magnetic Resonance Imaging (MRI) produces a multidimensional image of the brain that requires segmentation. However, this is a labor-intensive manual task that often exhibits significant inter-observer variability. Automated segmentation will therefore enable faster and more efficient tumor segmentation for accurate early identification of brain tumors. This study introduces the ResUNET segmentation network utilizing a Tversky loss function. It tackles class imbalance, a significant challenge in brain tumor segmentation. We surpass UNET in segmentation outcomes by addressing class imbalance and accurately segmenting the smaller, critical areas of the tumor. Our model achieves an intersection-over-union (IoU) score of 0.95 and a predicted Dice coefficient of 0.98 during testing, indicating a highly accurate match for expected tumor sites with a deviation of only 0.1 in placement. In other words, the tumor segmentation maps we predict reflect the size of the input images, making them both valid and significant. These results illustrate the progress our method has made in automating brain tumor segmentation, aiding in early diagnosis and treatment.**

***Index Terms*—Deep learning, MRI, Tversky loss, ResUNET, brain tumor segmentation, and biomedical imaging.**

I. Introduction

The human brain controls mental processes similarly to a central processing unit. However, aberrant tumor development, whether malignant or benign, may interfere with its regular function [1]. Because malignant tumors grow quickly, early detection is essential. MRI images, followed by manual segmentation, are the current approaches, which are labor-intensive and highly susceptible to human error. The current research shows that the ResUNET model, which combines deep learning with residual learning, might help identify and separate brain tumors more accurately and quickly. Convolutional neural networks play a vital role in segmenting brain tumors. Essentially, a CNN is a unique type of artificial neural network specifically developed to analyze data formatted in a grid-like structure, such as images. It may be feasible to derive useful information for brain tumor segmentation from medical imaging. An MRI scan or another form of medical imaging is the initial input that a CNN processes. Convolution involves systematically applying a series of filters, which are small grids, to an input image. Each filter detects specific elements or structures in the image, such as edges or textures. The CNN leverages its convolution mechanism to recognize and interpret complex structures within the input. The CNN continuously analyzes the input through convolution layers to identify relevant features for brain tumor segmentation. These are forwarded to the upper layers of the network for additional analysis. Essentially, the CNN improves the data by converting the raw input into a more abstract form, making it suitable for transmission through the network. A CNN model undergoes repeated exposure to a labeled dataset to train for the brain tumor segmentation challenge.

CNNs are designed to recognize key tumor characteristics, including size, shape, and location, by fine-tuning parameters to closely match the actual tumor segmentation. They excel more in classification tasks compared to segmentation. Consequently, the creation of the CNN-based UNET architecture emerges as a vital solution for segmentation. The UNET architecture is particularly effective for brain tumor segmentation. CNNs are designed to recognize key tumor characteristics like size, shape, and location by fine-tuning parameters to closely match accurate tumor segmentation. CNNs generally excel in classification tasks compared to segmentation tasks. Therefore, creating an architecture—the CNN-based UNET—is a crucial solution for segmentation. One very effective technique for brain tumor segmentation is the UNET architecture. Through the use of convolution to extract fine features, max pooling for down-sampling and concatenation to combine context and fine-grained data, its ”U” shape aids in the isolation of tumors from medical pictures [2]. To reduce feature map sizes without sacrificing important information, the UNET uses max pooling. To enable accurate

tumor border recognition in up-sampling, concatenation combines contextual characteristics from the contracting route with fine features from the expanding route. Lastly, up-sampling improves segmentation accuracy and offers a thorough description of the tumor by returning the feature maps to the original input picture dimensions. ResUNET is a variant on UNET, however. It is better than the conventional UNET design by using residual blocks and skip connections [3]. By removing vanishing gradients, adding residual and skip connections, accelerating convergence, and maintaining crucial early-layer information, the ResUNET expands on this. Res-UNET's skip connections preserve essential features and enhance gradient flow, resulting in accurate tumor segmentation and overall performance improvement. This research aims to investigate how the ResUNET architecture addresses the limitations of conventional methods, thereby improving the accuracy of brain tumor detection and segmentation. Consequently, the main objectives of this study are:

- Enhancing Brain Tumor Segmentation with ResUNet to Address Class Imbalance and Precisely Identify Small, Critical Diagnostic Areas.
- To assess the effectiveness of ResUNET against traditional CNN and UNET models for brain tumor detection.
- To verify how skip and residual connections enhance tumor edge detection, prevent vanishing gradients, and optimize gradient flow.

The rest of the paper is divided into three sections. Section III details the methodology and explains the proposed model comprehensively. Section IV follows with the results and discussions, offering a comparative analysis of various models. Finally, Section V concludes with a summary of the paper's findings.

II. Related Works

Brain tumor segmentation (BTS) has proven to be a productive research area, ranging from simple techniques to intricate deep-learning architectures. Numerous studies have presented new models aimed at enhancing segmentation efficiency and accuracy. The authors of [4] suggested a multifractal feature-based stochastic model, which increased segmentation accuracy but still needed work. By developing the ResUNET++ paradigm to solve gradient vanishing, the authors of [5] made a significant contribution. AGResU-Net, a U-Net architecture with residual modules and attention gates, was introduced by the authors in [6] to enhance small-scale tumor segmentation; nonetheless, challenges persist with complex pictures and small annotated datasets. The automated U-Net-based segmentation described by the authors in [7] was tested with BRATS 2015 and demonstrated good cross-validation; nevertheless, additional clinical validation is required. In [8], the authors presented a 3D picture segmentation method that addresses voxel imbalances using an objective function based on dice coefficients. This method is more efficient but mostly tends to binary segmentation. The authors of [9] used a 3D U-Net with weighted focal loss to address class imbalance in 3D brain MRIs; nonetheless, pixel degradation during training is still a problem. SVMs and Wavelet Transformers were investigated by Dan Lascu et al. [10] for the classification of tumors, with a deep learning option that needs to be optimised.U-Net was first presented by the authors [11] for semantic segmentation. Yang et al. [12] then added residual networks (ResU-Net) to improve feature extraction. HTTU-Net by Aboelenein et al. [13] for tumor segmentation on tiny scales, Group Cross Channel Attention U-Net by Huang et al. [14] to preserve low-level tumor features, and attention-based ResUNet by Zhang et al. [15] are additional innovations. Dou et al. [16] and Lee et al. [17] to achieve faster convergence and learning capacity. In general, the segmentation of brain tumors has significantly advanced thanks to advancements in deep learning, especially CNN-based models such as variations of U-Net. However, challenges remain, including precision concerns for small tumors, class imbalance, and data scarcity. This paper introduces a ResUNet model that employs the Tversky loss function to tackle these challenges, focusing on class imbalance and improving accuracy for small tumors.

Recent advancements in brain tumor segmentation utilize transformer architectures and attention mechanisms to address the limitations of traditional CNN methods. CNNs struggle to capture global feature relationships, affecting segmentation accuracy. This has led to Vision Transformers (ViTs), which effectively capture global information. The Focal Cross Transformer model [18] demonstrates the effectiveness of cross-window and focal self-attention mechanisms in multi-view brain tumor segmentation tasks. Many studies explore hybrid techniques integrating CNNs with attention mechanisms. The deformable attention and saliency mapping technique [19] showed promising results in classifying and segmenting multi-class MRI brain tumors. The ensemble attention mechanism [20] addresses the complexity of varying anatomical structures in MRI images through a novel dual-network feature extraction approach. A study of fifteen loss functions for brain CT segmentation found that the Focal Tversky and Tversky loss functions are the most effective, reinforcing our preference for Tversky loss. Recent research by Li et al. [21] introduced Region-related Focal Loss (RFL), which adapts gradients for difficult voxels. Additionally, compound loss functions integrating Dice with TopK, focal, and boundary loss show robustness in segmentation tasks [22].

Despite advancements, challenges remain in managing small tumor regions, ensuring cross-institutional generalization, and achieving computational efficiency. Our ResUNET method, using Tversky loss, addresses these challenges with residual learning and targets class imbalance.

III. METHODOLOGY AND EXECUTION

The process phases involve model construction, assessment, pre-processing, and data collection. This study develops two models: one for segmentation using ResUNET to define tumor borders, and another for classification to detect tumor presence.

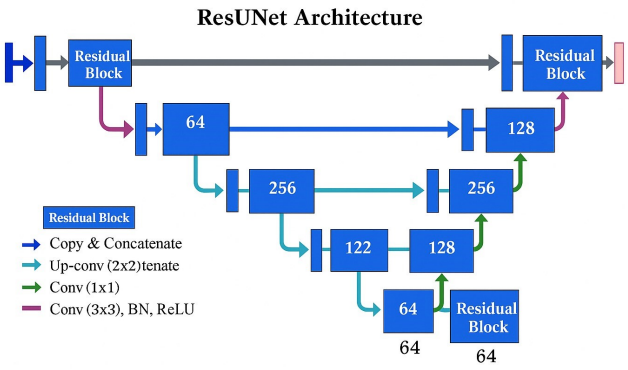

Fig. 1. A dual model system designed for detecting brain tumors using MRI

A. Data Collection and Pre-processing

The dataset contains 3,929 MRI images of brain tumors sourced from Kaggle.[1] Each image contains a binary mask indicating the tumor's location. The data sets for training and testing were divided in an 80:20 ratio. To identify missing values and analyze the distribution of binary labels (0 for no tumor, 1 for tumor), exploratory data analysis (EDA) was conducted. For better visibility, data visualization techniques like overlaying masks on MRI images were employed.

The Image Data Generator in TensorFlow/Keras facilitated data augmentation techniques, including random rotations, flips, and feature scaling. Besides being resized to match the model's input dimensions, the images were also normalized to a pixel intensity range of [0, 1] and underwent noise reduction processes.

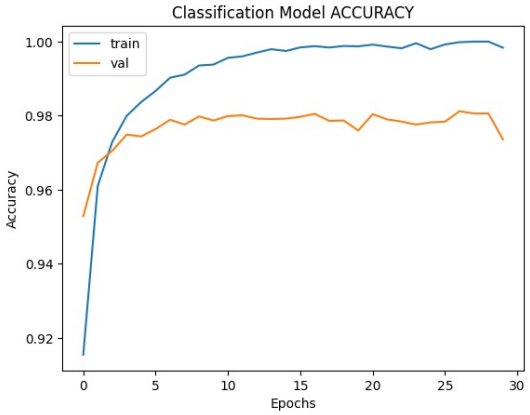

Fig. 2. Accuracy of the Classification Model

B. Model Architecture

The architecture of the proposed model is illustrated in Fig. 1. This classification model employs ResNet50, pre-trained on ImageNet, by incorporating custom layers like Average Pooling, Flatten, two Dense layers with ReLU activation, dropout layers, and a softmax output layer for binary classification. The ResUNET segmentation model incorporates ResNet residual blocks within the U-Net framework. The encoder consists of convolutional layers featuring max-pooling and ReLU activation, while the decoder utilizes information from the encoder to recover spatial resolution. The output layer produces a binary mask that highlights tumor locations.

[1]https://www.kaggle.com/datasets/mateuszbuda/lgg-mri-segmentation

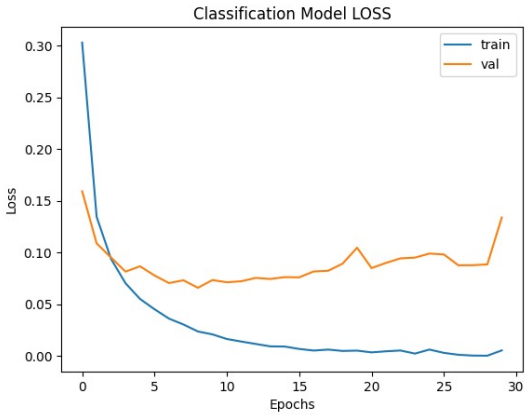

Fig. 3. Classification Model Loss

C. Training and Evaluation

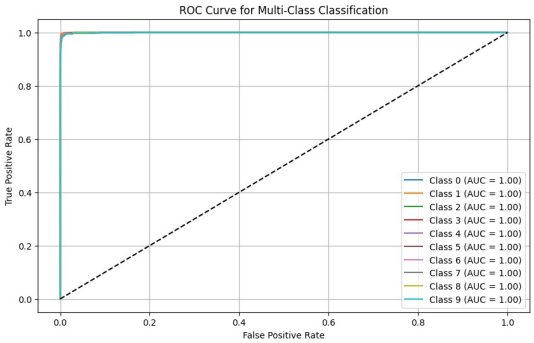

Fig. 4. ROC Curve for Multi-Class Classification

TABLE I
CLASSIFICATION METRICS

Metric	Formula and Value
Precision (%)	$\frac{TP}{TP+FP} \times 100\% = 99\%$
Recall (%)	$\frac{TP}{TP+FN} \times 100\% = 97\%$
F1-score (%)	$2 \times \frac{\text{Precision} \times \text{Recall}}{\text{Precision}+\text{Recall}} = 98\%$
Support	$\text{Support}(c) = \sum_{i=1}^{N} 1(y_i = c)$
Accuracy (%)	$\frac{TP+TN}{TP+TN+FP+FN} \times 100\% = 98\%$

Other border detection segmentation models are utilized once the classification model confirms the presence of a tumor. The process ceases if no tumor is detected. To maintain optimal model weights, training involved a generator-based approach with a batch size of 16, implementing early stopping when validation loss showed no improvement after 30 epochs. The evaluation of classification used the F1-score, recall,

accuracy, precision, and ROC curve. For segmentation, the overlap of the ground truth mask and predicted tumor borders was assessed using the intersection over union (IoU) and the Dice coefficient. The input and output process is depicted in Fig. 5.

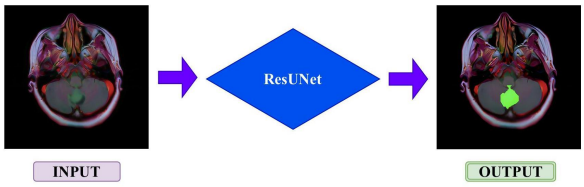

Fig. 5. Inputs and Outputs

D. Classification of Performance Metrics

Table IV showcases the exceptional performance of the classification model. To evaluate the model's capability in distinguishing between tumors and non-tumors, key metrics such as accuracy, precision, recall, and F1-score were defined. The model achieved 98% accuracy, 97% precision, 99% recall, and an F1-score of 98% for the non-tumor class (Label 0), while for the tumor class (Label 1), it attained 99% precision, 94% recall, and a 97% F1-score, reflecting its outstanding performance. Table IV summarizes these metrics, while Fig. 2 shows the training and validation accuracy curves, illustrating the model's convergence and high accuracy. The classification model loss and the ROC curve are presented in Fig. 3 and Fig. 4, respectively. Precise measurements of precision, recall, and F1-score are provided in Table IV, and Table V summarizes the overall classification model accuracy.

E. Performance Metrics for Segmentation

The evaluations using the Dice score and IoU demonstrated that the segmentation in the current study was very precise in outlining tumor boundaries. The Dice score can be calculated as follows:

$$\text{Dice} = \frac{2 \times |X \cap Y|}{|X| + |Y|} \tag{1}$$

In this context, X represents the predicted mask, while Y denotes the ground truth mask. The IoU is computed as follows:

$$\text{IoU} = \frac{|X \cap Y|}{|X \cup Y|} \tag{2}$$

These figures, together with the qualitative results shown in Fig. 6, demonstrate that the model effectively locates and defines tumor regions. With precise boundary identification across multiple samples, the AI-generated masks closely resemble the ground truth masks. A comparative analysis evaluated the new method in relation to established techniques, including 2D ResUNET, Multi-Inception, and 2D U-Net. The results presented in Table II indicate that the current methods excelled, achieving a Dice score of 0.98 and an IoU of 0.95. For additional evidence of the model's classification efficacy, refer to Fig. 7, which illustrates the true positives, true negatives, false positives, and false negatives in a clear manner. The confusion matrix reveals that the model correctly identified 350 non-tumor instances and 220 tumor instances, with only two false positives and six false negatives.

F. Final Model

To ensure precise tumor diagnosis and boundary delineation, our ultimate model, ResUNET, integrates ResNet's residual blocks with U-Net's segmentation accuracy. Better gradient flow and feature extraction are made possible by residual learning, which also increases the accuracy of tumor identification. A pipeline that combines classification and segmentation lowers computing complexity without sacrificing efficiency. For robustness and generalizability, sophisticated techniques are required. We employ data augmentation, early stopping, and model checkpointing techniques. ResUNET stands out as the most reliable, scalable, and precise system for medical image segmentation, achieving superior performance on metrics such as accuracy, IoU, and the Dice coefficient. The ResNet-50 classifier acts as a preliminary filter for detecting tumor presence. If no tumor is detected, the segmentation step is skipped, which helps save computational resources in large diagnostic processes. This two-step approach ensures both efficiency and precise effectiveness in clinical scenarios involving substantial image volumes. The classification stage serves as a filter, eliminating non-tumor images early in the process. This design boosts efficiency by invoking the segmentation model solely for relevant cases.

IV. Results and Discussion

ResUNET-based The proposed segmentation architecture performed better than previously reported. The model outperformed traditional architectures like CNN, ResUNet+, and U-Net++, achieving 0.98 Dice and 0.95 IoU scores. With a remarkable 98% classification accuracy, precision of 99%, recall of 97%, and F1-score of 98%, the model ensured highly accurate tumor detection. Comparative analysis revealed that ResUNET+ [5] enhances feature extraction via ROI-based segmentation, whereas SEResU-Net [15] and AGResU-Net [6] use attention mechanisms to enhance the identification of tiny tumors. Despite improvements, the models were unable to match ResUNET's segmentation accuracy and resilience when it came to matching projected tumor areas with ground

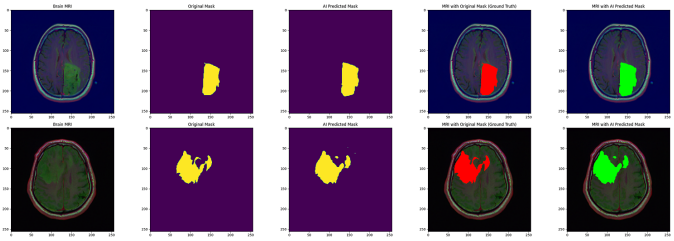

Fig. 6. Segmentation Outcomes (Original Image, Ground Truth Mask, AI-Predicted Mask)

TABLE II
COMPARATIVE EVALUATION OF BRAIN TUMOR SEGMENTATION RESEARCH

Study	Model Used	Dataset	Dice Score	IoU	Key Contributions
Our Proposed Method	ResUNET	Custom MRI dataset	0.98	0.95	Skip connections, strong feature extraction, and Tversky loss
Yan, Chengdong, et al. [15]	SEResU-Net (Residual + SE blocks)	BraTS2018, BraTS2019	0.9373 (Whole Tumor)	N/A	Better tiny tumor segmentation using an attention mechanism
Metlek, Sedat, and Halıt Çetıner. [5]	ResUNet+	BraTS2018, BraTS2019, BraTS2020	0.9280 (Whole Tumor)	N/A	Attention modules with ROI-based segmentation for improved feature extraction
Micallef, Neil, et al. [2]	U-Net++	BraTS2019	0.8712 (Whole Tumor)	N/A	Better post-processing and loss function methods
Zhang, Jianxin, et al. [6]	AGResU-Net (Attention + Residual)	BraTS2017, BraTS2018, BraTS2019	N/A	N/A	Attention gates enhance segmentation of small tumors
Ali, Mahnoor, et al. [9]	CNN + U-Net Ensemble	BraTS2019	0.906 (Whole Tumor)	N/A	CNN and U-Net combined in a hybrid model for increased accuracy

TABLE III
MATRIX OF CONFUSION

	Predicted 0	Predicted 1
Actual 0 (Negative Class)	True Negative (TN) = 350	False Positive (FP) = 2
Actual 1 (Positive Class)	False Negative (FN) = 6	True Positive (TP) = 220

TABLE IV
CLASSIFICATION REPORT FOR RESUNET-50

Label	Precision (%)	Recall (%)	F1-score (%)	Support
0	97	99	98	361
1	99	94	97	215
Accuracy	98 (576)			
Micro Avg	98	98	98	576
Macro Avg	98	97	97	576
Weighted Avg	98	98	98	576

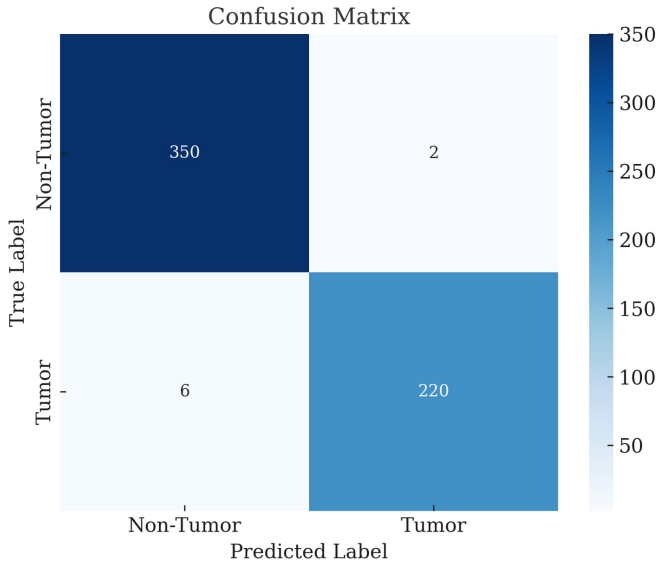

Fig. 7. Matrix of Confusion

TABLE V
THE CLASSIFICATION MODEL ACCURACY

Model	Accuracy
ResNet-50	98%

truth labels. matrix of confusion 7 Fig. validated the suggested model by confirming the presence of few false positives and false negatives. A clear classification report including the F1-score, precision, and recall for tumor and non-tumor classifications is given in Table IV. Fig. 6. shows the segmentation results graphically, with the AI-predicted tumor masks closely resembling the ground truth.Furthermore, the ROC curve Fig. 4 echoes the model's capacity to successfully distinguish between tumor and non-tumor regions, confirming the good classification performance with an AUC value of 1.00. A comparative analysis of different brain tumor segmentation models is presented in Table II, which also indicates the tendency towards improved performance of the suggested ResUNET model. With the highest Dice score (0.98) and IoU (0.95), the table demonstrates that ResUNET outperforms both the conventional U-Net and its variations. Some models, such ResUNet+ [5] and SEResU-Net [15], employ ROI-based segmentation and attention mechanisms to perform better on tiny tumor regions. However, their Dice scores are lower than ResUNET's, demonstrating the effectiveness of the suggested approach. The table also shows the trade-off between segmentation accuracy and model complexity, suggesting that advanced feature extraction techniques are necessary to improve performance. The findings confirm that ResUNET's Tversky loss function and residual blocks greatly improve segmentation accuracy while addressing the problems of poor boundary detection and class imbalance. For the cases of ResUNet+ [5] and SEResU-Net [15], the introduced model was more accurate; nevertheless, it would be modified based on attention mechanisms for subsequent tumor detection in the less frequent cases. Better generalization is provided by skip connections and residual blocks, which remove vanishing gradients and allow rich gradient propagation. Although the

CNN + U-Net [9] and U-Net++ [2] ensemble approaches produce competitive results, their higher computational complexity and lack of appreciable accuracy gains are due to their deeper model origins. Although the model demonstrates high accuracy on the Kaggle dataset, its generalizability across various clinical settings has yet to be evaluated. Future efforts will focus on testing the model with multi-institutional datasets to gauge its robustness and confirm its applicability in real-world clinical contexts. The ResUNET model is a strong contender for brain tumor segmentation since it achieves a compromise between computing efficiency and accuracy. For improved segmentation of difficult situations, such as small or overlapping tumors, future research needs to investigate integrating mechanisms of attention into ResUNET. A significant step towards the model's clinical applicability would be another use of it on sizable, multimodal data.

V. Conclusion

This research proposes a ResUNET model for brain tumor segmentation, enhancing identification speed. This architecture surpasses traditional UNET models by leveraging leftover blocks and skip connections, effectively addressing fading gradients for faster convergence and preserving spatial information, ultimately leading in better segmentation. With a dice value of 0.98 and an IoU score of 0.95, it outperforms both baseline and modified UNET models. To reduce human error and improve segmentation accuracy, the method incorporates precise preprocessing, classification, segmentation, and extensive data collection. It utilizes two models: a ResNet-50 classifier for tumor recognition and a ResUNET for segmentation. The Tversky loss function is applied during training to tackle class imbalance and improve performance in challenging scenarios.

In future studies, we will apply 5-fold or 10-fold cross-validation and incorporate external datasets for validation. This strategy ensures robustness and mitigates overfitting. We will also assess this dual-model approach's computational advantages and clinical feasibility, conducting model validation across various institutions and MRI modalities. Future research will explore the generalizability of this method for segmenting different types of cancer or organs using MRI images, utilizing larger and more diverse datasets to improve training and robustness. Furthermore, we will enhance the validity and strength of the proposed ResUNET architecture by investigating more complex topologies and tumor segmentation from 3D MRI volumes.

References

[1] A. Tiwari, S. Srivastava, and M. Pant, "Brain tumor segmentation and classification from magnetic resonance images: Review of selected methods from 2014 to 2019," *Pattern recognition letters*, vol. 131, pp. 244–260, 2020.

[2] N. Micallef, D. Seychell, and C. J. Bajada, "Exploring the u-net++ model for automatic brain tumor segmentation," *ieee Access*, vol. 9, pp. 125523–125539, 2021.

[3] N. Kaur and M. Sharma, "Brain tumor detection using self-adaptive k-means clustering," in *2017 international conference on energy, communication, data analytics and soft computing (ICECDS)*, pp. 1861–1865, IEEE, 2017.

[4] A. Islam, S. M. Reza, and K. M. Iftekharuddin, "Multifractal texture estimation for detection and segmentation of brain tumors," *IEEE transactions on biomedical engineering*, vol. 60, no. 11, pp. 3204–3215, 2013.

[5] S. Metlek and H. Çetıner, "Resunet+: A new convolutional and attention block-based approach for brain tumor segmentation," *IEEE Access*, 2023.

[6] J. Zhang, Z. Jiang, J. Dong, Y. Hou, and B. Liu, "Attention gate resunet for automatic mri brain tumor segmentation," *IEEE Access*, vol. 8, pp. 58533–58545, 2020.

[7] H. Dong, G. Yang, F. Liu, Y. Mo, and Y. Guo, "Automatic brain tumor detection and segmentation using u-net based fully convolutional networks," in *Medical Image Understanding and Analysis: 21st Annual Conference, MIUA 2017, Edinburgh, UK, July 11–13, 2017, Proceedings 21*, pp. 506–517, Springer, 2017.

[8] F. Milletari, N. Navab, and S.-A. Ahmadi, "V-net: Fully convolutional neural networks for volumetric medical image segmentation," in *2016 fourth international conference on 3D vision (3DV)*, pp. 565–571, Ieee, 2016.

[9] M. Ali, S. O. Gilani, A. Waris, K. Zafar, and M. Jamil, "Brain tumour image segmentation using deep networks," *Ieee Access*, vol. 8, pp. 153589–153598, 2020.

[10] M. Gurbină, M. Lascu, and D. Lascu, "Tumor detection and classification of mri brain image using different wavelet transforms and support vector machines," in *2019 42nd International Conference on Telecommunications and Signal Processing (TSP)*, pp. 505–508, IEEE, 2019.

[11] O. Ronneberger, P. Fischer, and T. Brox, "U-net: Convolutional networks for biomedical image segmentation," in *Medical image computing and computer-assisted intervention–MICCAI 2015: 18th international conference, Munich, Germany, October 5-9, 2015, proceedings, part III 18*, pp. 234–241, Springer, 2015.

[12] S. L. Lau, E. K. Chong, X. Yang, and X. Wang, "Automated pavement crack segmentation using u-net-based convolutional neural network," *Ieee Access*, vol. 8, pp. 114892–114899, 2020.

[13] N. M. Aboelenein, P. Songhao, A. Koubaa, A. Noor, and A. Afifi, "Httu-net: Hybrid two track u-net for automatic brain tumor segmentation," *IEEE Access*, vol. 8, pp. 101406–101415, 2020.

[14] H. Seo, C. Huang, M. Bassenne, R. Xiao, and L. Xing, "Modified u-net (mu-net) with incorporation of object-dependent high level features for improved liver and liver-tumor segmentation in ct images," *IEEE transactions on medical imaging*, vol. 39, no. 5, pp. 1316–1325, 2019.

[15] C. Yan, J. Ding, H. Zhang, K. Tong, B. Hua, and S. Shi, "Seresu-net for multimodal brain tumor segmentation," *IEEE Access*, vol. 10, pp. 117033–117044, 2022.

[16] P. Liu, Q. Dou, Q. Wang, and P.-A. Heng, "An encoder-decoder neural network with 3d squeeze-and-excitation and deep supervision for brain tumor segmentation," *IEEE Access*, vol. 8, pp. 34029–34037, 2020.

[17] J. Li, R. Zhang, L. Shi, and D. Wang, "Automatic whole-heart segmentation in congenital heart disease using deeply-supervised 3d fcn," in *International Workshop on Reconstruction and Analysis of Moving Body Organs*, pp. 111–118, Springer, 2016.

[18] L. Zongren, W. Silamu, F. Shurui, and Y. Guanghui, "Focal cross transformer: multi-view brain tumor segmentation model based on cross window and focal self-attention," *Frontiers in Neuroscience*, vol. 17, p. 1192867, 2023.

[19] E. Zarenia, A. A. Far, and K. Rezaee, "Automated multi-class mri brain tumor classification and segmentation using deformable attention and saliency mapping," *Scientific Reports*, vol. 15, no. 1, p. 8114, 2025.

[20] F. Celik, K. Celik, and A. Celik, "Enhancing brain tumor classification through ensemble attention mechanism," *Scientific Reports*, vol. 14, no. 1, p. 22260, 2024.

[21] B. Li, X. You, Q. Peng, J. Wang, and C. Yang, "Region-related focal loss for 3d brain tumor mri segmentation," *Medical physics*, vol. 50, no. 7, pp. 4325–4339, 2023.

[22] J. Ma, J. Chen, M. Ng, R. Huang, Y. Li, C. Li, X. Yang, and A. L. Martel, "Loss odyssey in medical image segmentation," *Medical image analysis*, vol. 71, p. 102035, 2021.